



Power Electronic Systems  
Laboratory

© 2018 IEEE

Proceedings of the 18th International Conference on Power Electronics and Motion Control (PEMC 2018),  
Budapest, Hungary, August 26-30, 2018

## **Sinusoidal Input Current and Average Speed Control of a Single-Phase Supplied Three-Phase Inverter Drive without Electrolytic Capacitor**

M. Haider,  
D. Bortis,  
J. W. Kolar,  
Y. Ono

Personal use of this material is permitted. Permission from IEEE must be obtained for all other uses, in any current or future media, including reprinting/republishing this material for advertising or promotional purposes, creating new collective works, for resale or redistribution to servers or lists, or reuse of any copyrighted component of this work in other works.



Eidgenössische Technische Hochschule Zürich  
Swiss Federal Institute of Technology Zurich

# Sinusoidal Input Current and Average Speed Control of a Single-Phase Supplied Three-Phase Inverter Drive without Electrolytic Capacitor

M. Haider, D. Bortis and J. W. Kolar  
Power Electronic Systems Laboratory,  
ETH Zürich, Switzerland  
Email: haider@lem.ee.ethz.ch

Y. Ono  
Nabtesco R&D Center,  
Nabtesco Corporation, Japan

**Abstract**—Single-phase supplied variable speed drives are mostly realized as two-stage systems comprising a single-phase PFC rectifier and a three-phase inverter stage. The intrinsic power pulsation of single-phase converters with twice the grid frequency is typically buffered by a bulky electrolytic DC-link capacitor, which is a major drawback concerning converter volume, costs and especially lifetime. Therefore, this paper presents a novel and simple implementation of a Machine-integrated Power Pulsation Buffer (MPPB) concept, which utilizes the inertia of the rotating mass as an energy storage to cover a part or the full input power pulsation. This allows to either reduce or even eliminate the electrolytic capacitor resulting in a smaller and cheaper converter system with increased lifetime. The proposed MPPB control concept is fully implemented in software, which means that only simple couplings are added to the control structure. Since the hardware remains unaffected, this concept can also be easily applied to already existing drive systems. In addition to the derivation of the control scheme, the proper operation of the MPPB is verified for steady-state and transient operation by circuit simulations.

## I. INTRODUCTION

In industry applications, electrical drive systems with a power level of several kilowatts are often supplied from the single-phase AC grid in order to keep the grid interface as simple as possible. This involves e.g. variable speed fans, blowers, pumps and local automation systems, which are typically comprising three-phase machines. Consequently, a power electronic system is required to convert the single-phase AC input voltage into a symmetrical three-phase voltage system, whose magnitude and frequency are adjusted in order to control the machine speed. Further on, the input current drawn from the single-phase AC grid is controlled to be proportional to the input voltage to achieve unity power factor operation.

Typically, these drive systems are realized as two-stage systems consisting of a single-phase PFC rectifier followed by a three-phase inverter, whereas for each converter stage different topologies can be used [1]–[3]. As an example, in Fig. 1(a), the circuit diagram of a widely used drive system consisting of an unidirectional single-phase boost PFC rectifier and a conventional three-phase voltage source inverter including the three-phase machine and the mechanical load is shown. Such system allows only a power flow from the grid to the mechanical load and thus recuperative braking (often not required) is not possible, and/or braking requires additional hardware, e.g. a brake chopper. Furthermore, due to the inherent input power pulsation with twice the grid frequency originating from the unity power factor operation of single-phase PFC rectifiers, and the constant power demand of

three-phase inverters, in general a large intermediate DC-link capacitor  $C_{DC}$  is used to compensate for the active power pulsation between the two stages (cf. Fig. 1(b)). Hence, in order to keep the amplitude of the DC-link voltage ripple  $\Delta v_{DC}$  small, i.e. typically limited to a certain percentage of the DC-link voltage  $v_{DC}$ , and consequently to provide a more or less constant voltage to the inverter stage, for medium-power applications a capacitance value  $C_{DC}$  in the mF-range is needed

$$C_{DC} = \frac{P_0}{2\omega_G} \cdot \frac{1}{\bar{V}_{DC}\Delta v_{DC}}, \quad (1)$$

( $\omega_G = 2\pi f_G$ , where  $f_G$  is the grid frequency) and therefore primarily is realized with electrolytic capacitors, which for this system turns out to be a major drawback concerning volume, cost and especially converter lifetime [4], [5].

In the literature different Power Pulsation Buffer (PPB) concepts, replacing the electrolytic capacitors, have been investigated in order to overcome the mentioned disadvantages. One possibility is to shift the active power pulsation away from the DC-link capacitor to an additional active PPB circuit, which is either connected in parallel or in series to the remaining DC-link capacitor [6]–[8]. Common to all these circuits, the PPB contains a buffer capacitor whose voltage is cycled with a large voltage ripple  $\Delta v_{C,max}$ , which according to (1) results in a much lower overall capacitance value. However, due to the additional PPB circuit, the realization effort and the complexity of the drive system is increased.

Instead of adding complexity to the drive system's electronics, the pulsating input power  $p_G$  can also be covered by the machine. Hence, the machine is no more operated with a constant output power, but the pulsating power is directly delivered to the machine ( $p_M = p_G$ ) and no power has to be buffered in the power electronic converter. In general, there are two ways to realize such so-called Machine-integrated Power Pulsation Buffer (MPPB). The first approach utilizes the machine inductance  $L_M$  as an energy storage ( $E_L = \frac{3}{4}L_M\hat{I}_M^2$ , where  $\hat{I}_M$  denotes the machine phase current amplitude) to buffer the power pulsation [9]. Hence, the machine currents  $i_M$  are adjusted in such a way that in addition to the current component which is needed to generate a constant mechanical torque, a reactive current component is superimposed to cover the input power pulsation. However, the machine inductance  $L_M$  mainly depends on the machine construction (slotted or slotless construction, placement of the magnets in the rotor, etc.) and especially for high-speed and highly-dynamic drive systems (servo motor applications) the machine inductance is

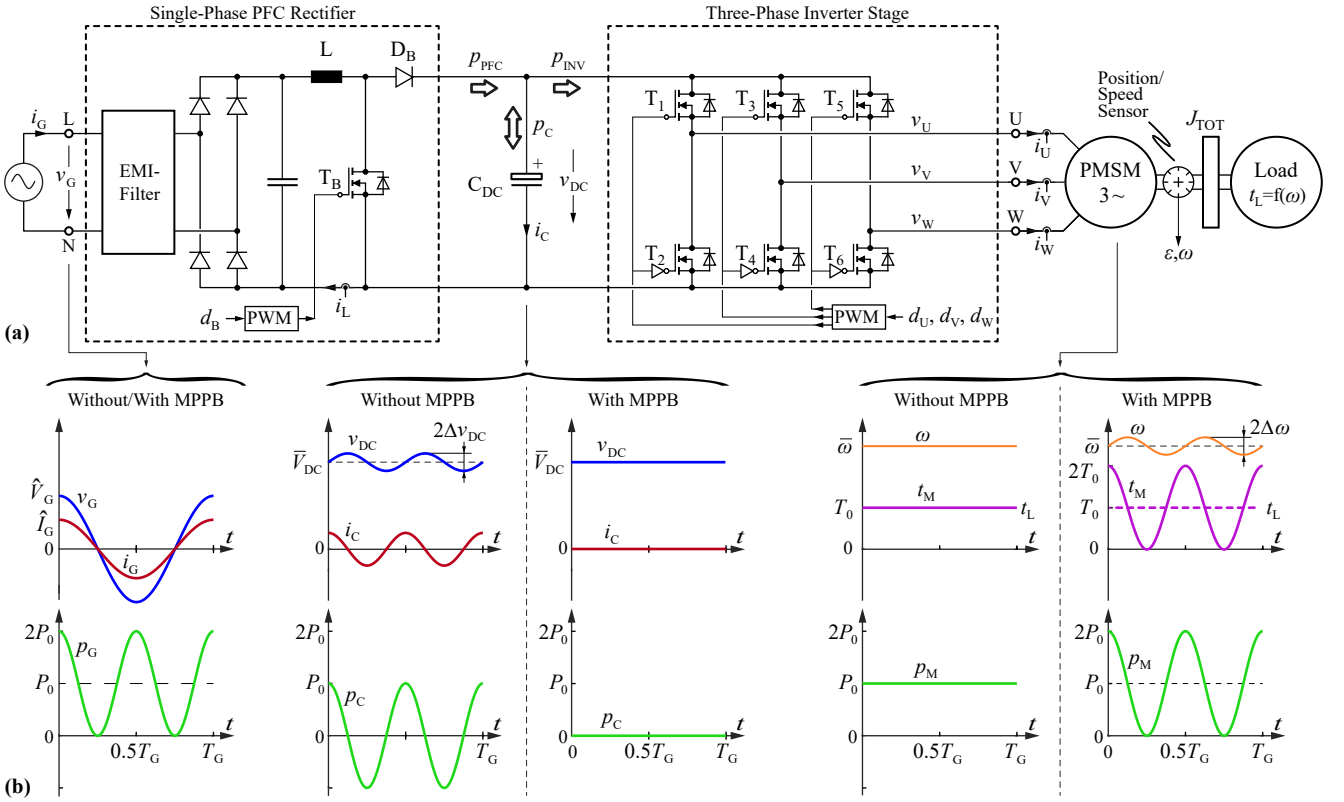


Fig. 1. (a) Circuit diagram of a conventional two-stage drive system implementation consisting of a single-phase PFC rectifier to achieve a sinusoidal input current and a three-phase inverter to operate the electrical machine with variable speed. The input power is typically buffered with an intermediate electrolytic DC-link capacitor  $C_{DC}$ . (b) Voltage and current waveforms at the grid, the DC-link and the machine obtained with and without Machine-integrated Power Pulsation Buffer (MPPB) visualized for one grid period  $T_G$  (switching frequency components omitted). Without the MPPB, the DC-link capacitor has to buffer the instantaneous power difference between PFC rectifier and inverter stage resulting in a voltage oscillation  $\Delta v_{DC}$  with twice the grid frequency  $2f_G$  at the DC-link. With the MPPB, the DC-link capacitor can (theoretically) be eliminated, since the pulsating input power is directly transferred to the machine, i.e. the machine is no more operated with a constant power leading to a pulsating machine torque  $t_M$  and rotational speed  $\omega$ .

small, which in turn would lead to a large reactive current component in case the full power pulsation should be buffered in the machine. As a consequence, due to the strongly increasing copper losses and the thermal limitation of the machine,  $i_M$  has to be restricted below a certain maximum value, which also limits the maximum stored energy  $E_{L,max}$  and finally increasingly constricts the power pulsation capability with higher machine torque and/or machine power. For this reason, the electrolytic capacitor is typically only reduced but not completely eliminated.

The second possibility to buffer the pulsating power in the machine, is to drive the machine directly with a pulsating mechanical output power ( $p_M = \omega \cdot t_M = p_G$ ). Consequently, this results in a pulsating torque  $t_M$  and a pulsating rotational speed  $\omega$  with twice the grid frequency (cf. Fig. 1(b)), whereas the amplitude of the speed ripple  $\Delta\omega$  is given as

$$\Delta\omega = \frac{P_0}{2\omega_G} \cdot \frac{1}{\bar{\omega} J_{TOT}}. \quad (2)$$

Within one mains period this means that if the instantaneous input power is larger than the average power, the machine is accelerated and excessive power is stored as kinetic energy ( $E_{KIN} = \frac{1}{2} \cdot J_{TOT} \omega^2$ ), and as soon as the input power drops below the average power, the machine is decelerated and stored kinetic energy is released again. In other words, in addition to the drive task, the machine is used as a kind of flywheel, e.g. as already used for peak power reduction in traction systems [10], [11], peak power supply within railway grids [12], smoothing of the output power of renewable power sources like wind

power [13], or within dynamic voltage restorers [14]. Due to the large moment of inertia  $J_{TOT}$  of low-speed systems or the high rotational speed  $\omega$  of high-speed machines, the stored kinetic energy of the mechanical system is typically orders of magnitudes larger than the required energy to buffer the electric power pulsation at the input, which in consequence leads to only a slight variation in the rotational speed  $\omega$  around its average value  $\bar{\omega}$ , but a large variation in the mechanical torque between zero and twice the average torque value with twice the grid frequency.

Therefore, due to the almost constant speed, this MPPB concept is still widely used in low-power, low-cost home appliances and hand tools employing conventional single-phase machines [15]–[18]. As another prominent and long-established application, the MPPB concept is also found in single-phase machine railway applications [19], which nowadays in general are replaced by three-phase machines. Even though, since in many countries the trains are supplied from a single-phase AC grid, the problem of pulsating input power and/or a large DC-link capacitor still exists, especially in railway applications where the grid frequency is lower than 50/60Hz. For this reason and also due to the simplicity of the described MPPB concept, which offers the possibility to reduce or even theoretically eliminate the DC-link capacitor, in this paper this MPPB concept is recaptured, improved and applied to standard single-phase supplied three-phase drive systems.

Actually, it has to be mentioned that the MPPB concept was already proposed for three-phase machines, where the

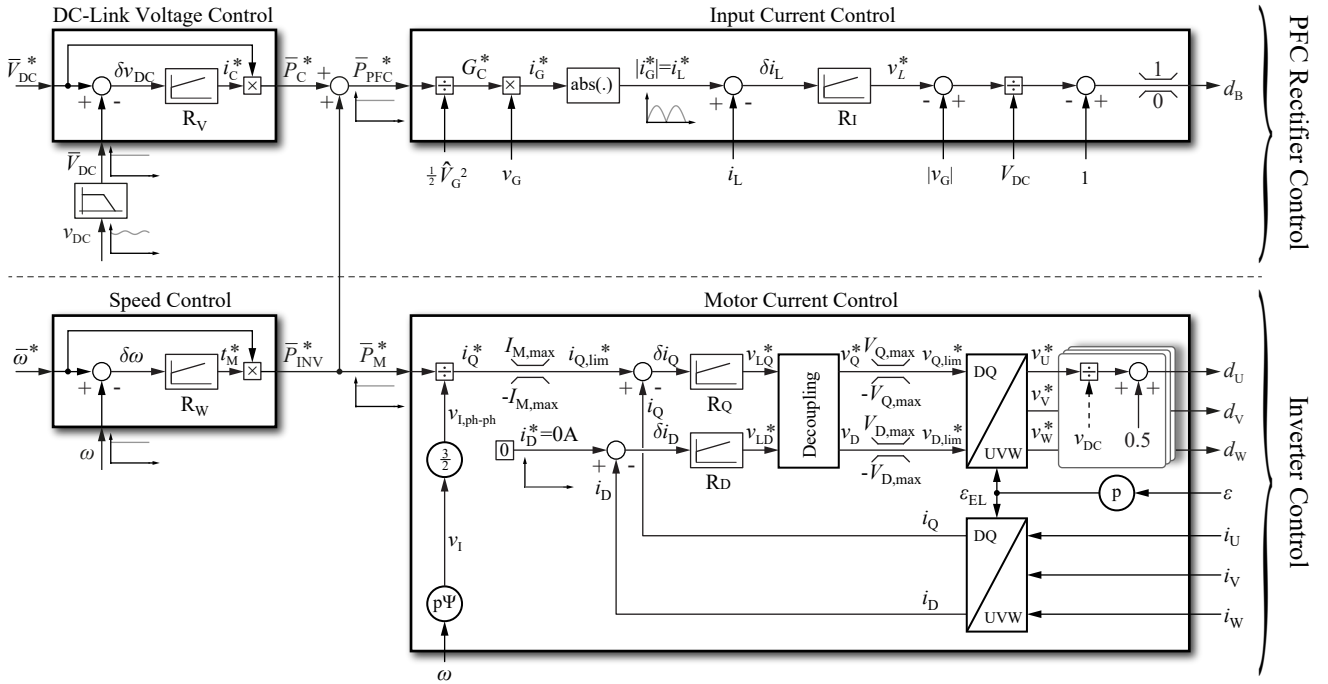


Fig. 2. Typical control structure of a conventional single-phase supplied drive system (cf. Fig. 1(a)) with mainly decoupled control structures for both the PFC rectifier and inverter stage. In order to achieve a high power/current quality at the input and high control dynamic at the output, the control structures of both stages are realized in a cascaded fashion.

PFC rectifier is omitted and the inverter stage is directly supplied from a single-phase grid via an input diode bridge rectifier [20]–[23]. As a major drawback, however, this concept features a rectified sine wave voltage at the DC-link, which means that the input current can only be controlled sinusoidally as long as the machine voltage stays below the rectified input voltage. Hence, either a machine with a low back EMF must be used or a large speed variation has to be accepted, but in both cases, a sinusoidal input current profile in the vicinity of the input voltage zero crossings is not possible to achieve and the PFC functionality is lost. In order to remedy this problem, in [24] this concept was extended by injecting a reactive current component into the machine such that the back EMF of the machine is always kept below the input voltage. Indeed, the PFC rectifier can now be omitted, however, as already mentioned, with a small machine inductance this concept leads to large machine currents and thus excessive losses. Furthermore, due to the fluctuating and low DC-link voltage, the complexity of the system is increased and the field of application is restricted to drive systems with special low-voltage machines, i.e. no standard machines and/or common machine voltages can be used.

The MPPB concept proposed in this paper differs therein that the MPPB concept is applied to standard single-phase supplied three-phase drive systems consisting of a conventional single-phase PFC rectifier followed by a three-phase inverter where the proposed MPPB extension is only realized in software by introducing simple couplings between the PFC rectifier and inverter control structures. Advantageously, the principle control blocks and structures remain unchanged, and also in the hardware no changes are required. Furthermore, in contrast to existing approaches, the proposed control scheme offers the possibility to not only distribute but also to define how the pulsating input power should be shared between DC-link capacitor and machine, i.e. the DC-link capacitor is not

fully eliminated but the current stress is reduced. One option is to operate the machine with a constant output power as long as the output power is low. The DC-link capacitor then buffers the total pulsating power. At higher output power, the machine is taking over the additional power pulsation and keeps the current stress at the capacitor constant. Another option is that in any operating point the machine buffers a certain share of the input power pulsation. This degree of freedom, which also depends on the application, the load characteristics and the mission profile of the drive system, can be used to increase the lifetime of e.g. already existing system and/or to design the DC-link capacitor in new systems for lower power ratings, i.e. to only provide, foil or ceramic capacitors in the extreme case.

Based on the conventional control structure of single-phase supplied drive systems, in **Section II** the proposed control concept with the insertion of the mentioned couplings is derived. In **Section III**, the influence of the distribution factor  $k$ , which defines the partitioning of the input power pulsation between DC-link capacitor and machine, is analyzed concerning current stress reduction in the capacitor and additional losses in the machine. The control concept is applied to a 7.5kW compressor drive system and the proper functionality of the MPPB concept is verified for steady-state and transient operation by circuit simulations, in **Section IV**. Finally, **Section V** summarizes the findings of the work and gives an outlook to future research.

## II. DERIVATION OF THE PROPOSED MPPB CONTROL SCHEME

In conventional single-phase supplied drive systems, the PFC rectifier and the inverter stage are decoupled by the intermediate DC-link capacitor and therefore also the control structures of both stages are mainly decoupled from each other. Furthermore, in order to achieve a high power/current quality at the input and high control dynamic at the output, typically



machine power  $p_M(t)$

$$\begin{aligned} p_M(t) &= \bar{P}_M + p_{M,AC} = \bar{P}_M + k \cdot p_{PFC,AC} \\ &= \bar{P}_{PFC} - \bar{P}_C + k \cdot (p_{PFC}(t) - \bar{P}_{PFC}) \\ &= k \cdot p_{PFC}(t) - \bar{P}_C + (1 - k) \cdot \bar{P}_{PFC}. \end{aligned} \quad (5)$$

Starting again from the conventional control, where only the averaged DC-link voltage  $\bar{V}_{DC}$  is used for the voltage controller and therefore the measured DC-link voltage  $v_{DC}(t)$  has to be low-pass filtered, with (5) the control structure in **Fig. 4** is found, where again the main control blocks are unchanged and only couplings between the rectifier and inverter control are added. There, the power distribution factor  $k$  is a degree of freedom and can be optimally and dynamically adapted to the underlying application with its given load characteristic and mission profile.

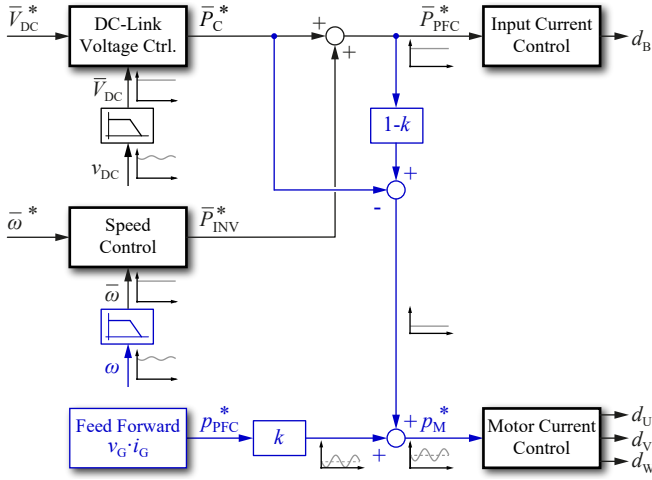


Fig. 4. Alternative control implementation with the possibility (compared to Fig. 3) to define the distribution of the pulsating input power between the DC-link capacitor and the machine with a distribution factor  $k \in [0, 1]$ , i.e. the fraction of the power pulsation which is covered by the machine  $p_{M,AC} = k \cdot p_{PFC,AC}$ .

### III. PERFORMANCE IMPACT OF THE POWER DISTRIBUTION FACTOR $k$

In the following the influence of the power distribution factor  $k$  on the system performance is analyzed. Since the distribution factor  $k \in [0, 1]$  defines the fraction of the pulsating input power which is covered by the machine, and the remaining part has to be buffered by the electrolytic capacitor, the equations of the instantaneous power at the rectifier ( $p_{PFC}(t)$ ), the inverter ( $p_{INV}(t)$ ), the machine ( $p_M(t)$ ) and the capacitor ( $p_C(t)$ ) are directly given as

$$p_{PFC}(t) = P_0 + P_0 \cos 2\omega_G t, \quad (6)$$

$$p_M(t) = p_{INV}(t) = P_0 + k P_0 \cos 2\omega_G t, \quad (7)$$

$$p_C(t) = p_{PFC}(t) - p_{INV}(t) = (1 - k) P_0 \cos 2\omega_G t. \quad (8)$$

Due to the fact that the magnitude of the pulsating capacitor power scales with the factor  $(1 - k)$ , i.e. changing  $P_0$  to  $(1 - k)P_0$  in (1), either the voltage ripple  $\Delta v_{DC}$  or the capacitor value  $C_{DC}$  can be reduced by the same factor  $(1 - k)$ , which in the latter case saves volume and costs.

In any case, to calculate the current in the capacitor, it can be assumed that the voltage ripple  $\Delta v_{DC}$ , which is typically limited by the application, is always much smaller than the nominal DC-link voltage  $\bar{V}_{DC}$ . Hence, the capacitor current  $i_C(t)$  can easily be found by dividing the instantaneous capacitor power  $p_C(t)$  given in (8) by the nominal DC-link voltage  $\bar{V}_{DC}$

$$i_C(t) = \frac{p_C(t)}{v_{DC}} \approx \frac{p_C(t)}{\bar{V}_{DC}} = \frac{P_0}{\bar{V}_{DC}} (1 - k) \cos 2\omega_G t. \quad (9)$$

In contrast to the decreasing magnitude of the capacitor power, the magnitude of the oscillating machine power linearly increases with  $k$  which means that in (2) the power  $P_0$  has to be substituted by  $kP_0$ , and therefore also the speed ripple  $\Delta \omega$  increases with  $k$ .

However, similarly as for the voltage ripple  $\Delta v_{DC}$ , the speed ripple  $\Delta \omega$  is still small compared to the average speed value  $\bar{\omega}$  due to the typically large moment of inertia  $J_{TOT}$ . Consequently, as already mentioned, this leads to a pulsating machine torque which according to  $t_M = \frac{p_M(t)}{\omega} \approx \frac{p_M(t)}{\bar{\omega}}$  has to be proportional to the instantaneous machine power  $p_M(t)$ .

Considering a symmetrical permanent magnet synchronous machine ( $L_D = L_Q$ ) and controlling the machine in the rotating dq-coordinate system (cf. **Fig. 2**), the mechanical torque  $t_M$  is only generated by the q-current component and due to this proportionality the torque-proportional current  $i_Q(t)$  is found as

$$i_Q(t) \approx I_{Q0} (1 + k \cos 2\omega_G t) \propto t_M. \quad (10)$$

The magnitude of the q-current is given by  $I_{Q0} = \frac{P_0}{\frac{3p}{2} \Psi_{PM} \bar{\omega}}$ , where  $p$  is the number of pole pairs and  $\Psi_{PM}$  equals the flux linkage of the permanent magnet rotor.

As one might expect, since now the q-current is pulsating with twice the grid frequency and therefore is no more constant as in the conventional case, the phase currents  $i_U$ ,  $i_V$  and  $i_W$  into the machine are no more purely sinusoidal. The corresponding phase currents can be calculated by transforming the q-current back to the stationary coordinate system (inverse Park transform), which for the phase current  $i_U = -i_Q \sin(p\bar{\omega}t + \varphi_0)$  is evaluated in (13). As can be noticed, the phase currents now contain two additional harmonic components located at the frequencies  $|2\omega_G + p\bar{\omega}|$  and  $|2\omega_G - p\bar{\omega}|$ , whereas their magnitudes scale proportionally to the power distribution factor  $k$ , and for this reason the phase current deviation from a sinusoidal shape (constant q-component of the machine current) increases with  $k$  as visualized in **Fig. 5**.

Based on the calculated time behaviour of the capacitor current  $i_C(t)$  and the phase currents  $i_{Ph}(t)$ , now the RMS-currents  $I_{C,rms}$  and  $I_{Ph,rms}$  can be determined, which in combination with the equivalent series resistance (ESR) of the capacitor  $R_{C,ESR}$  and the stator winding resistance  $R_{S,M}$  lead to the related losses  $P_{V,C}$  and  $P_{V,M}$ .

$$I_{C,rms} = \frac{P_0}{\bar{V}_{DC}} \frac{1 - k}{\sqrt{2}}, \quad P_{V,C} = R_{C,ESR} I_{C,rms}^2, \quad (11)$$

$$I_{Ph,rms} = \frac{P_0}{\frac{3p}{2} \Psi_{PM} \bar{\omega}} \frac{\sqrt{2 + k^2}}{2}, \quad P_{V,M} = 3R_{S,M} I_{Ph,rms}^2. \quad (12)$$

$$i_U(t) = -I_{Q0} (1 + k \cos 2\omega_G t) \sin(p\bar{\omega}t + \varphi_0) = -I_{Q0} \left[ \sin(p\bar{\omega}t + \varphi_0) + \frac{k}{2} \sin(2\omega_G t + p\bar{\omega}t + \varphi_0) - \frac{k}{2} \sin(2\omega_G t - p\bar{\omega}t - \varphi_0) \right] \quad (13)$$

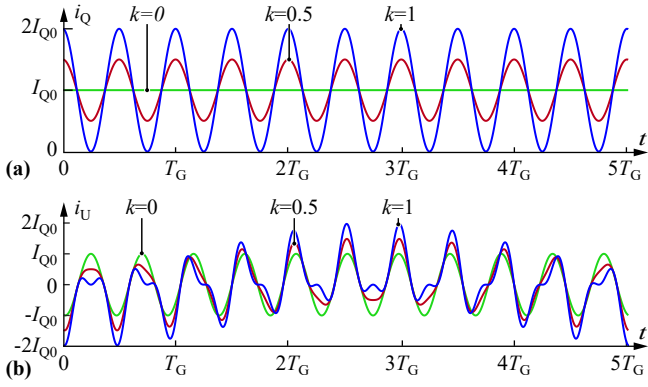


Fig. 5. Impact of the power distribution factor  $k$  on (a) the torque generating current  $i_Q$  and (b) the machine phase current  $i_U$ . The two additional harmonic components of the machine phase current scale linearly with  $k$  and are shown for  $p\bar{\omega} = 1.1 \cdot 2\omega_G$  with a grid frequency of 50 Hz and two pole pairs, i.e. the harmonics occur at 10 Hz and 210 Hz.

The machine RMS-current  $I_{Ph,rms}$  linearly increases, while the capacitor RMS-current  $I_{C,rms}$  linearly decreases with  $k$ . Consequently, the related losses show a quadratic behaviour proportional or inversely proportional to  $k$ . In Fig. 6, the loss dependency on  $k$  is shown for the normalized capacitor losses  $p_{V,C} = (1 - k)^2 P_0^2 / P_{0,N}^2$  and the normalized machine losses  $p_{V,M} = (1 + k^2/2) P_0^2 / P_{0,N}^2$ .

Starting from applications where the employment of electrolytic capacitors due to reliability or lifetime reasons is not allowed and thus the electrolytic capacitance has to be completely eliminated, the machine has to buffer the total pulsating input power, i.e. the electrolytic capacitor-less drive system is operated with  $k = 1$ . As can be noticed, due to the strong increase of the stator winding losses (where further loss components are neglected) - at full output power ( $P_0 = 100\%P_{0,N}$ ) the losses in the stator winding exceed the maximum losses by 50% - the machine either has to be oversized or can only be operated temporarily in this overload range due to thermal limitations. This, however, goes hand in hand with a large number of industrial applications where the drive systems are operated only during short time intervals, e.g. during start-up, transients, or acceleration phases at their nominal power  $P_{0,N}$ , while most of the time the systems are operated at reduced output power, e.g. within 70%-80% of  $P_{0,N}$  (grey shaded area). This also coincides with the results shown in Fig. 6, where the maximum allowed continuous output power for  $k = 1$  is 81% of  $P_{0,N}$ , which means that the machine losses are still kept below the maximum allowed continuous machine losses ( $p_{V,M} < 1$ ) and therefore all mentioned benefits, like DC-link voltage ripple reduction, capacitor volume decrease or lifetime enhancement of the MPPB concept can be applied.

In applications, where the continuous operating range has to be enlarged, the power distribution factor has to be limited to values below  $k = 1$ . For example, if a continuous operating range up to  $P_0 = 90\%P_{0,N}$  is needed, the distribution factor is limited to  $k = 0.68$ . Even in this case, however, the DC-link capacitance can be reduced by 68% which saves volume and costs. Furthermore, at low power operation (below 81%), during transients or based on the given mission profile, the power distribution factor can be dynamically increased up to  $k = 1$ , which means that in this case the losses in the electrolytic capacitor are diminishing or completely disappear. Hence, the lifetime of the remaining electrolytic capacitor is increased, since the lifetime of electrolytic capacitors doubles if the capacitor's core temperature is reduced by 10 K [28].

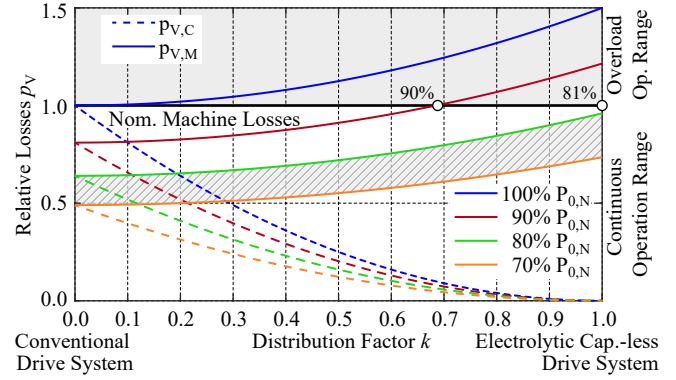


Fig. 6. Normalized capacitor losses  $p_{V,C} = (1 - k)^2 P_0^2 / P_{0,N}^2$  (dashed lines) and normalized machine losses  $p_{V,M} = (1 + k^2/2) P_0^2 / P_{0,N}^2$  (solid lines) for different output power levels (70%, 80%, 90% and 100% of the nominal power  $P_{0,N}$ , i.e. the maximum allowable continuous machine losses) as a function of the distribution factor  $k$ . The hatched area indicates the operation between 70% and 80%  $P_{0,N}$ . For  $k = 1$ , the maximum continuous output power is limited to 81%, while for  $k = 0.9$ , the continuous operating range is extended to 90%. Due to the increased losses and thermal limitations, the operation at higher output power levels (grey shaded area) is limited to only short time intervals, e.g. start-up or acceleration phases.

#### IV. VERIFICATION OF THE MPPB CONCEPT

The control and the operation of the proposed MPPB concept is verified with circuit simulations by means of a single-phase (230 V/50 Hz) supplied variable speed compressor drive system. According to Fig. 1, the system consists of a single-phase boost PFC rectifier, a three-phase inverter and a permanent magnet synchronous machine which drives a compressor with a nominal output power of 7.5 kW and a rotational speed of 3000 rpm. The overall system specifications are summarized in Tab. I and the circuit parameters are listed in Tab. II.

TABLE I  
SUMMARY OF THE DRIVE SYSTEM SPECIFICATIONS.

Grid voltage $V_{G,rms}$	230 V
Angular grid frequency $\omega_G$	$2\pi \cdot 50$ Hz
DC-link voltage $V_{DC}$	450 V
Maximal DC-link voltage ripple $\Delta v_{DC,max}$	$\pm 7.5$ V
Nominal mechanical power $P_{0,N}$	7.5 kW
Nominal rotational speed $n_N$	3000 rpm

TABLE II  
SUMMARY OF THE CIRCUIT PARAMETERS.

PFC boost inductance $L$	200 $\mu$ H
PFC switching frequency $f_{SW,PFC}$	140 kHz
PFC efficiency $\eta_{PFC}$	98%
Inverter switching frequency $f_{SW,INV}$	140 kHz
Inverter efficiency $\eta_{INV}$	98%
D-/Q-axis inductance $L_D/L_Q$	2 mH
Permanent magnet flux linkage $\Psi_{PM}$	275 mVs
Number of pole pairs $p$	2
Machine inertia $J_M$	1.1 mNm $s^2$
Machine efficiency $\eta_{PMSM}$	93%
Compressor inertia $J_L$	3.3 mNm $s^2$
Compressor efficiency $\eta_{COM}$	80%

Starting from a conventional drive system without MPPB, where the DC-link capacitor has to buffer the complete power pulsation, for the given specifications the DC-link capacitance has to be  $C_{DC,CS} = 4$  mF. The electrolytic capacitors needed to realize such a capacitance value typically feature an ESR of around  $R_{ESR} = 60$  m $\Omega$ , thus the capacitor losses at nominal

power are calculated to be  $P_{V,C}(k = 0) \approx 20$  W, which are much smaller than the nominal machine losses of  $P_{V,Mnom} = P_{0,N}(1 - \eta_{PMSM}) = 525$  W.

By implementing the proposed MPPB with  $k = 1$ , the electrolytic capacitor can be removed and only a small film or ceramic capacitor of  $C_{DC,II} = 30 \mu\text{F}$  is needed to handle the switching frequency current at the DC-link and to limit the voltage ripple below  $\Delta v_{DC,HF} = \pm 2$  V. The smaller DC-link capacitor has a major influence on the braking operation, as the intermediate voltage increases much faster during braking and results in a higher DC-link voltage ripple for a given brake chopper frequency. Accordingly, in order to keep the intermediate voltage still within its limits, the brake chopper is subject to a much higher switching frequency and thus its operation is not suitable anymore. Consequently, the only way to brake the machine electrically is by means of a bidirectional PFC rectifier, whereby the proposed control scheme is still suitable to deliver the recuperated power back to the grid (with increasing machine speed variation at lower speed values). The corresponding waveforms at nominal output power are shown in **Fig. 7(a)**. As can be noticed, the low-frequency DC-link voltage ripple almost disappears, however, now a speed ripple of  $\Delta n = \pm 89$  rpm ( $\pm 3\%$ ) occurs at the machine. Due to the system inertia, the torque  $t_M$  pulsates around the nominal torque of  $\bar{T}_M = 26.7$  Nm with a torque ripple of  $\Delta t_M = \pm 25.9$  Nm ( $\pm 97\%$ ). Furthermore, as already mentioned, at nominal load the stator winding losses increase by 50% and the continuous operation is limited to an output power of 81% of the nominal power  $P_{0,N}$ , if the worst case, where the stator losses equal the total machine losses, is assumed. Even though the machine losses strongly increase, the total system losses are only increased by +12%, since for the underlying application the overall efficiency  $\eta$  is mainly defined by the low compressor efficiency. Hence, the overall system efficiency  $\eta$  at nominal power only decreases from 71.5% ( $k = 0$ ) to 69% ( $k = 1$ ).

In order to extend the continuous operating range and thus to reduce the losses in the machine, the system can also be operated with a power distribution factor below  $k = 1$ . To point out a difference in the operation and the simulations, a distribution factor of  $k = 0.5$  is selected, which extends the continuous operating range to 94% of the nominal power  $P_{0,N}$  and increases the machine losses by 12.5% at nominal power. Compared to the case without MPPB, the total system losses of the underlying application only increase by 3%, which reduces the system efficiency to 70.8% ( $-0.7\%$ ). On the other hand, the DC-link capacitance can be decreased by 50% to  $C_{DC} = 2$  mF, which means that half of the capacitor volume, losses and costs can be saved. However, as shown in **Fig. 7(b)**, due to the power splitting between the DC-link capacitor and the machine, compared to  $k = 1$  now a voltage ripple of  $\Delta v_{DC} = \pm 7.5$  V and a reduced speed ripple of  $\Delta n = \pm 49$  rpm ( $\pm 1.6\%$ ) appears. Furthermore, with  $k = 0.5$  also the torque ripple is reduced to  $\Delta t_M = \pm 14.3$  Nm ( $\pm 54\%$ ) compared to  $k = 1$ . In case of the power pulsation splitting the feasibility of a brake chopper operation depends on the reduction of the DC-link capacitor. However, recuperative braking can be achieved with the same control structure but requires a bidirectional PFC rectifier in order to deliver the excessive power to the grid.

In addition to the steady state operation also the transient behaviour of the system is analyzed. Thereby, the distribution factor is increased again to  $k = 1$ , in order to verify the controller performance of the MPPB for the worst case

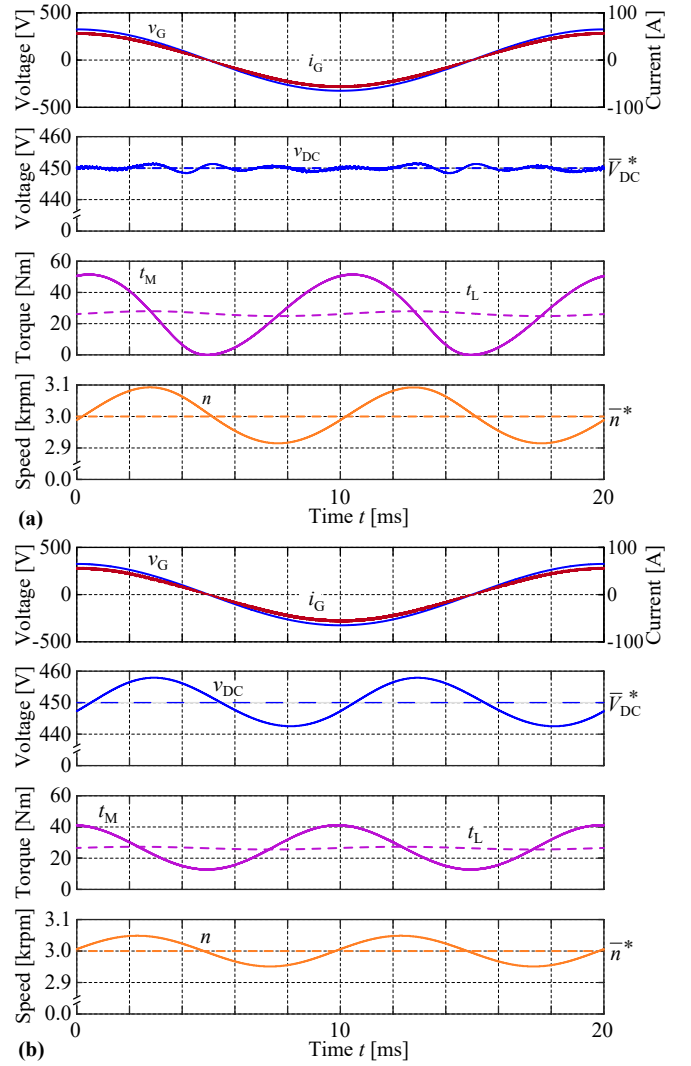


Fig. 7. Waveforms of the grid voltage  $v_G$  and current  $i_G$ , the DC-link voltage  $v_{DC}$ , the machine torque  $t_M$  and the rotational speed  $n$  during steady-state operation at nominal power for (a) the electrolytic capacitor-less drive system ( $k = 1$ ) and (b) the drive system with reduced DC-link capacitance ( $k = 0.5$ ).

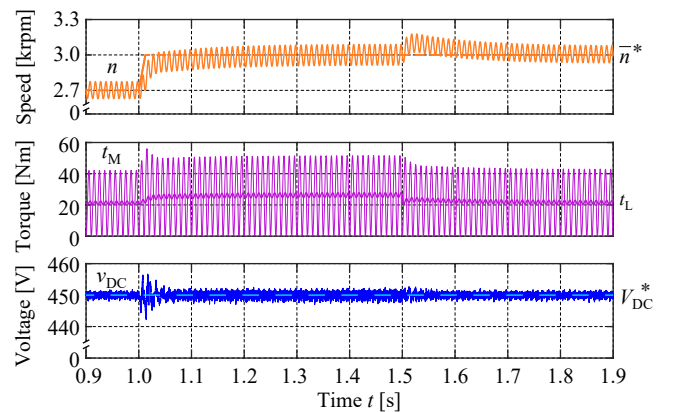


Fig. 8. Dynamic response of the proposed control structure for  $k = 1$  on a speed step at  $t = 1$  s and a load torque step at  $t = 1.5$  s. The reference speed  $\bar{n}^*$  as well as the speed  $n$ , the load  $t_L$  and the machine torque  $t_M$  as well as the DC-link voltage  $v_{DC}$  and its reference  $\bar{V}_{DC}^*$  are presented. For both steps, the system requires around 250 ms to reach the steady-state again.

with the smallest DC-link capacitance. In **Fig. 8** the transient behaviour for a speed step from  $\bar{n}^* = 2.7$  krpm to  $\bar{n}^* = 3.0$  krpm with  $\frac{dn}{dt} = \frac{480 \text{ rpm}}{20 \text{ ms}}$  at  $t = 1$  s and a load torque step from  $t_L = 24$  Nm to  $t_L = 19.2$  Nm at  $t = 1.5$  s is shown. For

both excitations, the system requires around 250 ms to reach the steady-state again, whereas the disturbances at the DC-link voltage  $v_{DC}$  are almost negligible.

## V. CONCLUSION

This paper proposes a novel and simple implementation of a Machine-integrated Power Pulsation Buffer (MPPB) concept for single-phase supplied variable speed drives. Thereby, the inertia of the rotating mass is utilized as energy storage to buffer the inherent power pulsation caused by the unity power factor operation of the PFC rectifier. In order to utilize only the machine as power pulsation buffer or to distribute the power pulsation between the DC-link capacitor and the machine, two different control structures are derived and the proper operation is verified by simulations for steady-state and transient behaviour. The performance impact of the power pulsation factor, which defines the fraction of the power pulsation covered by the machine, is analyzed. It results that if the total pulsating input power is buffered by the machine, the losses in the machine increase, thus the continuous output power range reduces to 81% of the nominal output power due to thermal limitations of the machine. By reducing the share of the pulsating power in the machine, also the losses decay and the continuous output power range can be extended. Furthermore, at lower output power, the share of the pulsating power in the machine can be dynamically increased without strongly deteriorating the system efficiency, which further reduces the power pulsation in the DC-link capacitor and therefore leads to longer lifetime of the employed electrolytic capacitors as presented for two application scenarios of a compressor drive system.

## ACKNOWLEDGMENT

The authors would like to express their sincere appreciation to Nabtesco Corp., Japan, for the financial and technical support of research on Advanced Mechatronic Systems at the Power Electronic Systems Laboratory, ETH Zurich. Furthermore, inspiring technical discussions with K. Nakamura are especially acknowledged.

## REFERENCES

- [1] J. S. Moghani and M. Heidari, "High efficient low cost induction motor drive for residential applications," in *Proc. of the International Symposium on Power Electronics, Electrical Drives, Automation and Motion (SPEEDAM)*, Taormina, Italy, May 2006, pp. 1399–1402.
- [2] I. Çadirici, S. Varma, M. Ermis, and T. Gülsoy, "A 20 kW, 20 kHz unity power factor boost converter for three-phase motor drive applications from an unregulated single-phase supply," *IEEE Transactions on Energy Conversion*, vol. 14, no. 3, pp. 471–478, Sept. 1999.
- [3] C. B. Jacobina, E. C. Dos Santos, N. Rocha, and E. L. L. Fabricio, "Single-phase to three-phase drive system using two parallel single-phase rectifiers," *IEEE Transactions on Power Electronics*, vol. 25, no. 5, pp. 1285–1295, Jan. 2010.
- [4] M. L. Gasperi, "Life prediction model for aluminum electrolytic capacitors," in *Proc. of the 31st Industry Applications Conference (IAS)*, San Diego, CA, USA, Oct. 1996, pp. 1347–1351.
- [5] A. M. Imam, T. G. Habetler, R. G. Harley, and D. M. Divan, "Condition monitoring of electrolytic capacitor in power electronic circuits using adaptive filter modeling," in *Proc. of the 36th IEEE Power Electronics Specialists Conference (PESC)*, Recife, Brazil, June 2005, pp. 601–607.
- [6] D. Neumayr, D. Bortis, and J. W. Kolar, "Ultra-compact power pulsation buffer for single-phase DC/AC converter systems," in *Proc. of the 8th IEEE International Power Electronics and Motion Control Conference (ECCE)*, Hefei, China, June 2016, pp. 2732–2741.
- [7] R. Ghosh, M. Srikanth, R. Mitova, M. X. Wang, and D. Klikic, "Novel active ripple filtering schemes used in little box inverter," in *Proc. of the International Exhibition and Conference for Power Electronics, Intelligent Motion, Renewable Energy and Energy Management (PCIM)*, Nuremberg, Germany, May 2017, pp. 1–8.
- [8] S. Qin, Y. Lei, C. Barth, W. C. Liu, and R. C. N. Pilawa-Podgurski, "A high power density series-stacked energy buffer for power pulsation decoupling in single-phase converters," *IEEE Transactions on Power Electronics*, vol. 32, no. 6, pp. 4905–4924, Aug. 2017.
- [9] J. Kim, I. Jeong, K. Lee, and K. Nam, "Fluctuating current control method for a PMSM along constant torque contours," *IEEE Transactions on Power Electronics*, vol. 29, no. 11, pp. 6064–6073, Jan. 2014.
- [10] B. Szabados and U. Schaible, "Peak power bidirectional transfer from high speed flywheel to electrical regulated bus voltage system: A practical proposal for vehicular technology," *IEEE Transactions on Energy Conversion*, vol. 13, no. 1, pp. 34–41, Mar. 1998.
- [11] M. I. Daoud, A. S. Abdel-Khalik, A. Elserougi, S. Ahmed, and A. M. Massoud, "DC bus control of an advanced flywheel energy storage kinetic traction system for electrified railway industry," in *Proc. of the 39th IEEE Conference of the Industrial Electronics Society (IECON)*, Vienna, Austria, Nov. 2013, pp. 6596–6601.
- [12] M. L. Sough, D. Depernet, F. Dubas, B. Boualem, and C. Espanet, "PMSM and inverter sizing compromise applied to flywheel for railway application," in *Proc. of the Vehicle Power and Propulsion Conference (VPPC)*, Lille, France, Sept. 2010, pp. 1–5.
- [13] F. Diaz-Gonzalez, F. D. Bianchi, A. Sumper, and O. Gomis-Bellmunt, "Control of a flywheel energy storage system for power smoothing in wind power plants," *IEEE Transactions on Energy Conversion*, vol. 29, no. 1, pp. 204–214, Dec. 2014.
- [14] L. Zhou and Z. Qi, "Modeling and simulation of flywheel energy storage system with IPMSM for voltage sags in distributed power network," in *Proc. of the International Conference of Mechatronics and Automation*, Changchun, China, Aug. 2009, pp. 5046–5051.
- [15] S. P. Syrigos and E. C. Tatakis, "An alternative universal motor drive with unity power factor operating in DC and AC modes," in *Proc. of the 22nd IEEE International Conference on Electrical Machines (ICEM)*, Lausanne, Switzerland, Sept. 2016, pp. 962–9685.
- [16] D. Anton, K. Namsu, K. Youngkwan, and L. Seungmoo, "Substitution of the universal motor drives with electrolytic capacitorless PMSM drives in home appliances," in *Proc. of the 9th IEEE International Power Electronics and Motion Control Conference (ECCE-Asia)*, Seoul, South Korea, June 2015, pp. 1631–1637.
- [17] M. Chomat and T. A. Lipo, "Adjustable-speed drive with single-phase induction machine for HVAC applications," in *Proc. of the 32nd IEEE Power Electronics Specialists Conference (PESC)*, Vancouver, Canada, June 2001, pp. 1446–1451.
- [18] D. C. Huynh, B. H. Dinh, M. W. Dunnigan, T. A. T. Nguyen, and N. H. Le, "Parameter estimation of a single-phase induction machine using a dynamic particle swarm optimization algorithm," in *Proc. of the IEEE Power Engineering and Automation Conference (PEAM)*, Wuhan, China, Sept. 2011, pp. 183–186.
- [19] A. Steimel, *Elektrische Triebfahrzeuge und ihre Energieversorgung (in German)*. Munich, Germany: Deutscher Industrie-Verlag GmbH, 2014.
- [20] K. Inazuma, K. Ohishi, and H. Haga, "High-power-factor control for inverter output power of IPM motor driven by inverter system without electrolytic capacitor," in *Proc. of the IEEE International Symposium on Industrial Electronics (ISIE)*, Gdansk, Poland, June 2011, pp. 619–624.
- [21] H. S. Jung, S. J. Chee, S. K. Sul, Y. J. Park, H. S. Park, and W. K. Kim, "Control of three-phase inverter for AC motor drive with small DC-Link capacitor fed by single-phase AC source," *IEEE Transactions on Industry Applications*, vol. 50, no. 2, pp. 1074–1081, Nov. 2014.
- [22] I. Takahashi and H. Haga, "Power factor improvement of single-phase diode rectifier by fast field-weakening of inverter driven IPM motor," in *Proc. of the 4th IEEE International Conference on Power Electronics and Drive Systems*, Denpasar, Indonesia, Oct. 2001, pp. 241–246.
- [23] J. H. Tau and Y. Y. Tzou, "PFC control of electrolytic capacitor-less PMSM drives for home appliances," in *Proc. of the IEEE International Symposium on Industrial Electronics (ISIE)*, Edinburgh, UK, June 2017, pp. 335–341.
- [24] G. Wang, N. Zhao, J. Qi, C. Li, and D. Xu, "High power factor control of IPMSM drive system without electrolytic capacitor," in *Proc. of the 8th IEEE International Power Electronics and Motion Control Conference (ECCE-Asia)*, Hefei, China, May 2016, pp. 379–383.
- [25] J. J. Cabezas, R. Gonzalez-Medina, E. Figueres, and G. Garcera, "Comparison and combination of digital controls for single-phase boost PFC converters in avionic power systems," in *Proc. of IEEE International Symposium on Industrial Electronics (ISIE)*, Edinburgh, UK, June 2017, pp. 645–650.
- [26] T. Rudnicki, R. Czerwinski, and D. Polok, "Performance analysis of a PMSM drive with torque and speed control," in *Proc. of IEEE International Conference Mixed Design of Integrated Circuits and Systems (MIXDES)*, Torun, Poland, June 2015, pp. 562 – 566.
- [27] C. Hanju, V. Trung-Kien, J. Qi, and K. Jae-Eon, "Design and control of proportional-resonant controller based photovoltaic power conditioning system," in *Proc. of IEEE Energy Conversion Congress and Exposition (ECCE-USA)*, San Jose, CA, USA, Sept. 2009, pp. 2198–2205.
- [28] S. G. Parler, "Deriving life multipliers for electrolytic capacitors," Cornell Dubilier, Tech. Rep., 2004. [Online]. Available: <http://mexico.newark.com/pdf/tech/articles/cornellmultipliers.pdf>